MICROCOPY RESOLUTION TEST CHART
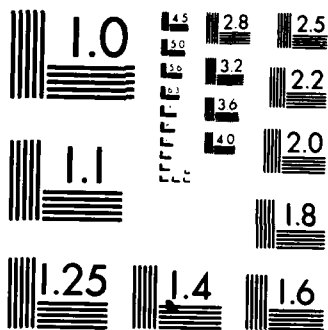
NATIONAL BUREAU OF STANDARDS 1963 A

OFFICE OF NAVAL RESEARCH

Contract N00014-79-C-0647

"HYDROGEN BONDED AND NON-HYDROGEN BONDED vdWs CLUSTERS:

COMPARISON BETWEEN CLUSTERS OF PYRAZINE, PYRIMIDINE

AND BENZENE WITH VARIOUS SOLVENTS"


by


J. Wanna, J.A. Menapace and E.R. Bernstein


Prepared for Publication

in the

Journal of Chemical Physics


Department of Chemistry
Colorado State University
Fort Collins, Colorado  80523


*1 JUNE* ~~May~~ 1986

AD-A172 348

# REPORT DOCUMENTATION PAGE

| 1a. REPORT SECURITY CLASSIFICATION | 1b RESTRICTIVE MARKINGS |
|---|---|
| 2a. SECURITY CLASSIFICATION AUTHORITY | 3. DISTRIBUTION/AVAILABILITY OF REPORT<br>Approved for public release; distribution unlimited. |
| 2b. DECLASSIFICATION/DOWNGRADING SCHEDULE<br>Unclassified | |

| 4. PERFORMING ORGANIZATION REPORT NUMBER(S)<br>N00014-79-C-0647 | 5. MONITORING ORGANIZATION REPORT NUMBER(S) |
|---|---|

| 6a. NAME OF PERFORMING ORGANIZATION<br>Colorado State University | 6b OFFICE SYMBOL<br>(If applicable) | 7a. NAME OF MONITORING ORGANIZATION |
|---|---|---|

| 6c. ADDRESS (City, State, and ZIP Code)<br>Department of Chemistry<br>Fort Collins, Colorado 80523 | 7b ADDRESS (City, State, and ZIP Code) |
|---|---|

| 8a. NAME OF FUNDING/SPONSORING ORGANIZATION<br>U.S. Army Research Office | 8b OFFICE SYMBOL<br>(If applicable) | 9 PROCUREMENT INSTRUMENT IDENTIFICATION NUMBER<br>N00014-79-C-0647 |
|---|---|---|

| 8c. ADDRESS (City, State, and ZIP Code)<br>Post Office Box 12211<br>Research Triangle Park, NC 27709 | 10 SOURCE OF FUNDING NUMBERS | | | |
|---|---|---|---|---|
| | PROGRAM ELEMENT NO | PROJECT NO. | TASK NO | WORK UNIT ACCESSION NO |
| | | | | |

**11. TITLE (Include Security Classification)**
"Hydrogen Bonded and Non-Hydrogen Bonded van der Waals Clusters: Comparison Between Clusters of Pyrazine, Pyrimidine, and Benzene with Various Solvents"

**12. PERSONAL AUTHOR(S)**
J. Wanna, J.A. Menapace, and E.R. Bernstein

| 13a. TYPE OF REPORT<br>Technical Report | 13b. TIME COVERED<br>FROM _____ TO _____ | 14. DATE OF REPORT (Year, Month, Day)<br>June 1, 1986 | 15 PAGE COUNT<br>43 |
|---|---|---|---|

**16. SUPPLEMENTARY NOTATION** The view, opinions, and/or findings contained in this report are those of the author(s) and should not be construed as an official Department of the Army position, policy, or decision, unless so designated by other documentation.

| 17. | COSATI CODES | | 18 SUBJECT TERMS (Continue on reverse if necessary and identify by block number) |
|---|---|---|---|
| FIELD | GROUP | SUB-GROUP | |
| | | | |
| | | | |

**19. ABSTRACT (Continue on reverse if necessary and identify by block number)**

Solute-solvent clusters of pyrazine, pyrimidine and benzene (solutes) and $C_nH_{(2n+2)}$ (n=1, 2), $NH_3$ and $H_2O$ (solvents) are studied by the techniques of supersonic molecular jet spectroscopy and two-color time of flight mass spectroscopy (2-color TOFMS). Spectral shifts, van der Waals (vdW) modes, dissociation energies, and vdW mode-solute mode vibronic couplings are characterized for most of the observed clusters. Based on these data and previous results for hydrocarbon systems, cluster geometries can be suggested. Lennard-Jones potential (6-12-1) calculations are also performed for these clusters and in all instances for which comparisons can be readily made, calculated and experimentally estimated geometries and binding energies agree completely. Clusters of N-heterocyclic solutes and $H_2O$ are not observed experimentally. Systematics and trends among the clusters reported herein and those previously reported are discussed and analyzed.

| 20 DISTRIBUTION/AVAILABILITY OF ABSTRACT<br>☒ UNCLASSIFIED/UNLIMITED ☐ SAME AS RPT ☐ DTIC USERS | 21 ABSTRACT SECURITY CLASSIFICATION<br>UNCLASSIFIED | |
|---|---|---|
| 22a NAME OF RESPONSIBLE INDIVIDUAL<br>Elliot R. Bernstein | 22b TELEPHONE (Include Area Code)<br>303-491-6347 | 22c OFFICE SYMBOL |

**DD FORM 1473, 84 MAR**     83 APR edition may be used until exhausted     SECURITY CLASSIFICATION OF THIS PAGE
All other editions are obsolete.

86     9

## I. Introduction.

Supersonic molecular jet spectroscopy has made possible the study of a wide variety of weakly bound, solute-solvent van der Waals (vdW) clusters in the gas phase. Cluster investigations have enhanced our understanding of intra- and intermolecular interactions and potentials, vibrational energy dynamics and chemical reactions, structural properties of small aggregates of solute and solvent molecules, and nucleation and growth of small clusters. Clusters can also be considered as model systems for condensed phase behavior. Moreover, these vdW systems can be thought of as an important new state of matter in which the static and dynamic properties of small aggregates of weakly coupled molecules can be studied.

vdW clusters, after being produced in a supersonic jet expansion, can be probed by three distinct techniques: fluorescence excitation (FE), dispersed emission (DE), and two-color time of flight mass spectroscopy (2-color TOFMS). The latter technique is employed most often in our studies of clusters because it gives unique cluster identification, brackets the cluster binding energies, and elucidates cluster vibrational energy dynamics and vibrational predissociation.

In the past few years, we have reported several studies of vdW clusters using the three spectroscopic techniques mentioned above.[1-7] Cluster geometry, binding energy, nucleation and growth dynamics, and limits on the vibrational energy dynamics and vibrational predissociation times have been determined. The vdW solute-solvent clusters investigated initially are for the most part restricted to aromatic hydrocarbon solutes (e.g., benzene and toluene) and small alkane solvents ($CH_4$, $C_2H_6$, and $C_3H_8$) in which only one type of interaction, that is one potential form, is found to be important for the solute-solvent coordination. Expanding on these previous studies we are now exploring solute-solvent clusters with N-heterocyclic solutes (e.g.,

1

pyrazine and pyrimidine) and alkane solvents and N-heterocyclic solutes with hydrogen bonding solvents (e.g., water and ammonia). The initial report of this effort for pyrazine and methane, ethane and propane clusters has already appeared.[7]

In this paper we discuss the 2-color TOFMS study of pyrimidine clustered with $CH_4$ and $C_2H_6$, pyrazine and pyrimidine clustered with $NH_3$, and benzene clustered with $H_2O$ and $NH_3$. The pyrimidine-alkane clusters are presented for comparison with the previously published[7] pyrazine-alkane data: the effect of the ring nitrogen atoms on the cluster geometry can thereby be evaluated. The pyrazine and pyrimidine ammonia clusters reveal the role of hydrogen bonding interactions in simple clusters. Benzene-water and-ammonia clusters serve as an example of clusters with these more complicated solvent systems (i.e., two possible interaction potentials) interacting with aromatic hydrocarbons. Theoretical and experimental studies of such a series of systems should eventually lead to a fuller understanding of solute-solvent coordination structure, dynamics, and the hydrogen bonding interaction.

Although extensive efforts were made and a wide variety of experimental conditions explored, pyrazine and pyrimidine clusters with water were not observed. Both FE and 2-color TOFMS detection techniques were employed. A broad feature (roughly 50 $cm^{-1}$ FWHM) was observed in FE at 580 $cm^{-1}$ to the blue of pyrazine $0_0^0$ transition for pyrazine and water expanded with helium. No signal, however, was observed at the pyrazine water mass channel for 2-color TOFMS. We must thus conclude that the pyrazine and pyrimidine water clusters have not been observed. Either the excited $n\pi^*$ state of the cluster is dissociative or internal conversion or intersystem crossing is so rapid for these clusters that the lifetime of the $n\pi^*$ state is greatly reduced (ca. 0.1 ps). Pyrimidine-fluorinated alcohol clusters also exhibit broad features and reduced lifetimes.[5]

Hydrogen bonding interactions are known to play an important role in intra- and intermolecular interactions important for secondary and tertiary molecular structure, molecular dynamics, and ionic and molecular solvation. Hydrogen bonding interactions have received attention in previous supersonic molecular jet spectroscopic studies: these systems include phenol clustered with various proton accepting molecules,[9] indole and 2-aminopyridine clustered with various solvents,[10] benzoic acid dimers,[11] s-tetrazine dimers,[12] 1,4-dihydroxyanthraquinone,[13] and methylsalicylate.[14] In most instances blue shifted cluster spectra are found due to the cluster stabilization of the ground state and destablization of the excited state.[15]

In this and our other cluster studies, the experimental data are supplemented by potential energy Lennard-Jones (LJ) atom-atom (6-12-1) calculations of cluster structure, binding energy, and internal motion. The calculations and the potential are discussed thoroughly in our previous studies.[7] The LJ calculations produce identical geometries but slightly lower binding energies than the exp-6 potential form used in earlier calculations.[1-6] The LJ hydrogen bonding (LJ-HB) potential form proves to be more versatile than the exp-6 form since many more constants for different types of atom-atom interactions have been independently reported for the LJ potential.[16] None of the potential parameters employed in this work is fit to the cluster data.

As is well known and widely accepted, geometries of isolated molecules and clusters are best obtained through spectroscopic observation of rotational structure. In fact, rotational structure of a number of simple clusters has been observed under molecular jet conditions: s-tetrazine and iodine with He and Ar[17] and aniline with Ne and Ar.[18] The resolution available to us at present is 0.06 cm$^{-1}$; at this resolution only rotational envelopes are observable which do not lend themselves readily to a unique interpretation of cluster structure. We calculate that 0.005 cm$^{-1}$ resolution would be required to

resolve rotational structure for $C_4H_4N_2(NH_3)_1$ etc., under the restriction
of a rigid geometry. We are thus for the present forced to employ less direct
methods to obtain cluster geometry. Assignment of the spectra is accomplished
through the determination of ionization energies, spectral shifts, relative
intensities, (molecular) symmetry forbidden cluster transitions, and potential
calculations. The understanding of these more complex systems rests heavily
on the previous data obtained for other clusters.[1-7] For all systems dis-
cussed in this paper, complete agreement between spectroscopic data, calculations
and results for previously analyzed solute-solvent clusters is found.

II.    Experimental Procedures.

The experimental apparatus and procedures are similar to those used
previously for the study of vdW clusters. The vacuum system consists of two
chambers with a pulsed nozzle and mass detection system in the second chamber.
A skimmer separates the pulsed nozzle and the time of flight mass spectrometer.
The first chamber contains either a pulsed or CW nozzle the molecular beam
from which can be taken into the second chamber through a skimmer. FE and DE
experiments are carried out in the first chamber.

The two independent lasers used in the 2-color TOFMS experiments are
$Nd^{+3}$/YAG pulsed lasers the doubled output of which pumps two dye lasers.
The dye laser output can be mixed with the 1.064 μm $Nd^{+3}$/YAG fundamental,
frequency mixed and doubled, or just doubled using various nonlinear KDP
crystals. The laser output can be extended from greater than 4.5 μr to
~0.215 μm. One laser is employed to excite the cluster to its first excited
$n\pi^*$ or $\pi\pi^*$ electronic state and the second laser then ionizes this cluster
starting from the $S_1$ vibronic manifold. The maximum ionization energy
achievable with this second laser is roughly 46,500 $cm^{-1}$.

The solute or cluster chromophore is typically placed in an inline trap
or filter cup directly behind the pulsed valve. Water is placed in a trap

before the valve and solute; the helium carrier gas passes over both materials and into the valve. Gaseous solvents are premixed with the helium carrier gas in a holding tank (~2000 psi) at concentrations varying from 2.0 to 0.1 mole/ mole percent.

The LJ potential function (6-12-1) with the additional HB form is described in detail in a previous publication.[7] Table I contains a list of the previously unreported constants employed with this potential form. Pyrazine and pyrimidine structures used in the calculations are obtained from reference 19.

III. Results.

This section contains the experimental and calculational results for the various clusters investigated. We first present pyrimidine with methane and ethane for comparison with the previously reported pyrazine clusters.[7] Pyrimidine and pyrazine ammonia clusters are then discussed and benzene water and ammonia clusters are presented for a comparison with the N-heterocyclic systems. Based on previous experience with a number of different clusters,[1-7] we have not made an extensive experimental study of the binding energies of these clusters. We rely on the calculations which have always fallen within the range bracketed by the experimental 2-color TOFMS data. Preliminary checks made on both pyrazine and pyrimidine clusters are in agreement with the calculations. Vibrational vdW modes observed in the spectra will not be assigned in this publication. Future publications will assign them as bends, stretches, torsions and combinations utilizing a normal coordinate calculational analysis.[20]

A. Pyrimidine - methane.

Figure 1 and Table II present the data for the pyrimidine $(CH_4)_1$ and $(CH_4)_2$ complexes taken near the pyrimidine $0_0^0$ transition (31073.0 $cm^{-1}$). The cluster of pyrimidine $(CH_4)_1$ has a spectral shift of -56.6

5

$cm^{-1}$ and a low frequency mode at 4.5 $cm^{-1}$ from this origin. These spectra are obtained by 2-color TOFMS. Hints of other vdW modes can also be seen in the trace in figure 1 but we are hesitant to report such weak transitions. Pyrimidine $(CH_4)_2$ spectra clearly show two clusters, similar to previously reported clusters for other aromatic systems.[1-7] The feature at -112.1 $cm^{-1}$ in figure 1 is assigned as the $0_0^0$ transition of the isotropic (symmetric), additive shift cluster and the feature at -47.2 $cm^{-1}$ is attributed to the $0_0^0$ transition of the anisotropic (asymmetric) cluster with both methanes on the same side of the aromatic ring. Note that without both mass and energy resolution, the spectra of pyrimidine $(CH_4)_1$ and $(CH_4)_2$ would not be resolved and the clusters could not be separated and uniquely identified. A vdW mode at 5.1 $cm^{-1}$ from the isotropic cluster origin is observed.

Potential energy calculations using LJ potentials for these clusters generate geometries and binding energies comparable to those previously reported for other aromatic-alkane systems and in complete accord with the above experimental findings (see fig. 2). Calculations for pyrimidine $(CH_4)_1$ clusters yield only one geometry for which the methane is coordinated with the aromatic π-system of the pyrimidine ring. The calculated binding energy for this cluster is 514 $cm^{-1}$. The methane carbon atom is above the ring at 3.5 Å and is shifted ~0.1 Å from the ring center toward the nitrogen atoms. The three hydrogen atoms of methane that point down toward the ring are equidistant from the ring at 3.1 Å; two of these hydrogens point directly at the ring nitrogen atoms. Again in agreement with the main experimental observations for these clusters, the calculations for pyrimidine $(CH_4)_2$ clusters yield two distinct geometrical arrangements. The isotropic cluster has a calculated binding energy of 1029 $cm^{-1}$ and the anisotropic cluster has a calculated binding energy of 879 $cm^{-1}$.

6

B.  Pyrimidine - Ethane.

The pyrimidine $(C_2H_6)_1$ spectrum is quite complicated, consisting of a number of low intensity features and an intense feature at -60.7 $cm^{-1}$ with respect to the pyrimidine origin (see figure 3). We might expect that little vdW vibronic intensity would be observed, based on pyrazine and other pyrimidine clusters. In order to begin to interpret these features we must consult the vapor phase room temperature pyrimidine monomer spectrum.[21] In these reports, features at -156 $cm^{-1}$ and +22 $cm^{-1}$ are assigned as the $16a_1^1$ and $16b_1^1$ sequence bands, respectively. The feature that appears in figure 3 at -39.1 $cm^{-1}$ may be assigned as the $16b_1^1$ sequence band of the pyrimidine $(C_2H_6)_1$ cluster built on the intense -60.7 $cm^{-1}$ cluster origin. If this identification is correct, then the clusters of pyrimidine $(C_2H_6)_1$ are hot $(T_{vib} \approx 260 \text{ K})$ and the features in figure 3 and table II at -153.5, -99.3, -86.9, and -75.4 $cm^{-1}$ may well be hot bands associated with the cluster origins at -71.4, -60.7 and -52.7 $cm^{-1}$. Apparently the cluster formation process for pyrimidine ethane tends to warm the cluster. Table III summarizes these results.

Supersonic expansion of pyrimidine apparently does not produce the expected cooling for vibrational modes $16b_1$ and $16a_1$. Vibrational temperatures for the $16b_1$ mode have been reported to be in excess of 200 K. Ito and coworkers[21d] have also observed the $16b_1^1$ transition for pyrimidine clustered with argon and nitrogen. In the present work, changes in backing pressure from 10 to 120 psi do not change the relative band intensities: apparently these modes present a bottleneck for vibrational cooling.

As can be seen in figure 4, three different configurations are calculated to be stable for the pyrimidine $(C_2H_6)_1$ cluster. Configuration I has the long axis of ethane perpendicular to the plane of the pyrimidine ring. Configurations II and III have the ethane molecule long axis more or less

7

parallel to the plane of the ring; for configuration II, the axis of ethane lies between a nitrogen and a carbon and for configuration III this axis lies between two carbon atoms. In each instance a $CH_3$-group lies more or less over the ring center.

C. Pyrimidine - Ammonia.

The pyrimidine $(NH_3)_1$ 2-color TOFMS spectrum in the range 300 to 500 $cm^{-1}$ to the blue of the pyrimidine origin is presented in figure 5. The three features are associated with the $0_0^0$ transitions of the pyrimidine $(NH_3)_1$ clusters. The lack of significant vdW vibrational mode intensity indicates that the ground and excited state vdW potentials are nearly identical. The large cluster blue shift implies a strong hydrogen bonding interaction between the pyrimidine and the ammonia. The spectrum of figure 5 is taken with an ionization energy of 45,110 $cm^{-1}$; lowering the ionization energy to ca. 42,000 $cm^{-1}$ the two nearly degenerate features at +367 $cm^{-1}$ decrease in intensity much more rapidly than the feature at +496 $cm^{-1}$. Table IV gives the energies and assignments for the pyrimidine $(NH_3)_1$ clusters. Based on the idea that the three features in this spectrum are associated with three different pyrimidine $(NH_3)_1$ cluster geometries, the two nearly isoenergetic configurations must be quite similar. The feature at +496 $cm^{-1}$ must correspond to a different (more hydrogen bonded) geometry.

Three different configurations are calculated for the pyrimidine $(NH_3)_1$ cluster using the LJ-HB potential form (see Table I and Reference 7). Two of these configurations have the ammonia above the pyrimidine plane and the third configuration has the $NH_3$ molecule not above the ring. These clusters are presented in figure 6 along with the calculated cluster binding energies. Configuration I has the ammonia N-atom 3.2 Å above the pyrimidine ring with the three ammonia hydrogen atoms pointing down toward the $\pi$-cloud. The two closest hydrogen atoms of the ammonia in this configuration are 2.7 Å from the pyrimi-

8

dine plane. In configuration II, the ammonia N-atom is 3.2 Å above the ring
plane and points in the general direction of the ring N-atoms. The closest two
ammonia H-atoms to the ring are at 2.7 Å. This cluster has a somewhat lower
binding energy than cluster I (667 $\underline{vs}$ 689 $cm^{-1}$). In the third pyrimidine
$(NH_3)_1$ configuration, the ammonia molecule does not reside over the pyrimidine
ring: the $NH_3$ has a N-H bond in the plane of the pyrimidine ring with the H-
atom pointing to one of the pyrimidine nitrogens, 2.23 Å from it. The ammonia
nitrogen is displaced in the xy plane by 3.3 Å and 2.8 Å along the x-axis and
y-axis respectively, as shown in figure 6, configuration III. This configura-
tion has a calculated binding energy of 537 $cm^{-1}$.

D. Pyrazine - Ammonia.

The pyrazine $(NH_3)_1$ spectra in the $0_0^0$, $10a_0^1$ and $6a_0^1$
regions are presented in figure 7. One first notices the significant dif-
ference between these data and those of pyrimidine $(NH_3)_1$. The spectra
all strongly suggest that only one configuration is present for the pyrazine
$(NH_3)_1$ system. The intense feature in the $0_0^0$ spectrum is the cluster
origin at +117 $cm^{-1}$ from the pyrazine $0_0^0$ transition. The remaining
features of this spectrum are vdW vibrational modes of the cluster. They
will be analyzed in a future publication.[20] Table V gives the energies and
the features observed in the spectrum. In this case, the ground and excited
state potential surfaces must be significantly different.

The cluster $10a_0^1$ transition is quite different from the cluster $0_0^0$ or
$6a_0^1$ transitions. From this one concludes that strong vdW-internal mode
coupling exists for the $10a^1$ out of plane ring mode.[22] The vdW overtones
and combination bands extend to more than 180 $cm^{-1}$ from the $10a_0^1$ cluster
origin feature. This is particularly striking in comparison with the $6a_0^1$
vibronic band.

9

Only one configuration is calculated for the pyrazine $(NH_3)_1$ cluster using the LJ plus HB potential function, in agreement with expectations from the spectra. The ammonia molecule hydrogen bonds to the ring nitrogens, through two ammonia hydrogens. The nitrogen atom of the ammonia molecule is 3.2 Å above the ring plane with all three hydrogens pointing toward the ring. This geometry is depicted in figure 8. The calculated binding energy of the cluster is 677 cm$^{-1}$.

E. Benzene - Ammonia.

The origin and $6_0^1$ transitions of the $C_6H_6(NH_3)_1$ cluster are observed in 2-color TOFMS. One can immediately conclude that at least one configuration of this cluster does not retain the benzene 3-fold axis. The spectra are traced in figure 9. The spectra for both transitions are far more complicated than any other cluster previously reported from our laboratory. Regions with similar structure can be found in the $0_0^0$ and $6_0^1$ spectra; in particular, the regions around +20 cm$^{-1}$, -20 cm$^{-1}$ and -60 cm$^{-1}$ in each spectra bear some resemblance to one another. Nonetheless, features appearing in one spectrum do not appear in the other, and therefore at least two clusters of different geometry are probably responsible for the $6_0^1$ transition. The $0_0^0$ transition could arise from one reduced symmetry cluster. Since very little a priori spectroscopic analysis seems possible in this situation at the present time, great stock must be placed in the calculations.

Two different configurations are calculated for the $C_6H_6(NH_3)_1$ cluster and both of them have the $NH_3$ molecule placed over the ring. Configuration I in figure 10 preserves the benzene $C_3$ axis and configuration II does not. The high symmetry cluster has the N-atom 3.3 Å from the ring plane and the three H-atoms of $NH_3$ are 2.9 Å above the ring plane. Configuration II has the N-atom 3.3 Å above the plane and slightly shifted from the ring

10

center. Two H-atoms of the $NH_3$ point towards C-C bonds and one points away from the ring plane. The $NH_3$ H-atoms in this configuration are at 2.9 Å (two of them) and 4.3 Å from the ring. The calculated binding energies of these two configurations are given in figure 10. Configuration II alone must generate the $0_0^0$ spectrum in figure 9.

F. Benzene - Water.

The $C_6H_6(H_2O)_1$ cluster $0_0^0$ and $6_0^1$ spectra are presented in figure 11. They are strikingly different from those of $C_6H_6(NH_3)_1$ (figure 9) but bear a strong resemblance to the pyrazine $(NH_3)_1$ spectra displayed in figure 7, as well as spectra of other systems studied in our laboratory.[1-7] In particular, a very clear vibronic progression is present for the $0_0^0$ spectrum and will be analyzed in a future publication.[20] Table VI gives these features and their energies. The $6_0^1$ spectrum of $C_6H_6(H_2O)_1$ has a different shift (+50 vs +85 cm$^{-1}$) and a different general pattern than the $0_0^0$. In addition, the $6_0^1$ origin is split by roughly 1 cm$^{-1}$. Considerable vibronic coupling must occur between thé in plane carbon-carbon stretch $6^1$ and the vdW modes. The $C_6H_6(H_2O)_1$ cluster 2-color TOFMS spectra are observed only at a higher ionization energy than required to observe the $6_0^1$ spectrum of bare $C_6H_6$. The $C_6H_6(H_2O)_1$ spectra depicted in figure 11 are taken with an ionization laser energy of 44,480 cm$^{-1}$ compared to 36,100 cm$^{-1}$ for the benzene monomer. The ionization energy for the benzene water cluster is 3300 cm$^{-1}$ higher than that of the benzene monomer.

Only one geometry is calculated for the $C_6H_6(H_2O)_1$ cluster employing the LJ potential. The configuration and binding energy are given in figure 12. The oxygen atom of water is roughly centered over the ring at 3.2 A above it and the water hydrogen atoms are at 3.0 Å above the ring. The calculated water benzene binding energy is 505 cm$^{-1}$.

11

## IV. Discussion

Cluster geometry is determined through analysis of 2-color TOFMS data for individual clusters and through calculations of cluster geometry and binding energies using an augmented LJ potential. Calculated binding energies have always been roughly bracketed by the experimentally observable range defined by two solute molecule vibrations (e.g., 520 to 850 $cm^{-1}$ for the 1:1 complex).[1-7]

Before discussing the details of the clusters observed, some general remarks are in order. First, one should take note of the great apparent differences between the spectra of the various clusters studied: pyrazine and pyrimidine hydrocarbon spectra show little vdW vibronic structure but intense origins; the pyrazine $(NH_3)_1$ spectrum displays elaborate and well developed vibronic progressions with a +117 $cm^{-1}$ cluster shift for a single cluster; the pyrimidine $(NH_3)_1$ spectra consist only of intense origins for three large shift (+366, +368, +496 $cm^{-1}$) configurations with no vdW vibronic development; the benzene $(NH_3)_1$ spectra are red shifted, and too complex to interpret without further calculations; and the benzene $(H_2O)_1$ spectra are blue shifted with extensive vdW structure. Second, and perhaps even more astonishing, the LJ-HB (where appropriate) potential calculations parallel and reinforce these differences in all cases. That is, for example, the calculations suggest one hydrogen bonded configuration for pyrazine $(NH_3)_1$ but three hydrogen bonded configurations for pyrimidine $(Nh_3)_1$, in agreement with the straight-forward interpretation of the spectra. Third, the binding energies of the clusters seem relatively insensitive to the detailed configuration of the cluster. Fourth, spectral shifts are found to be a sensitive function of the detailed geometry of the cluster. Proximity to the $\pi$-system is important for cluster red shifts, while hydrogen bonding yields in general cluster blue shifts with respect to the solute monomer origin.

12

A. Pyrimidine - Methane.

In the pyrimidine $(CH_4)_1$ cluster the $CH_4$ molecule is situated above the pyrimidine ring coordinated to the $\pi$-cloud of the aromatic ring. The cluster has a simple spectrum with little vdW vibronic intensity following the pyrimidine vibronic origins. The cluster spectrum is red shifted, indicating that the excited state cluster is more tightly bound than the ground state cluster by roughly 60 $cm^{-1}$. The overall appearance of the spectrum is similar to that of pyrazine methane.[7]

The additive shift features in the spectrum of pyrimidine $(CH_4)_2$ are attributed to the isotropic (symmetrical) geometry with a methane molecule on either side of the pyrimidine ring. The feature at -47.2 $cm^{-1}$ in the pyrimidine $(CH_4)_2$ spectrum is attributed to the anisotropic configuration with both $CH_4$ molecules on the same side of the ring. In this asymmetric geometry, one methane is more or less above the ring, and responsible for most of the $CH_4$-$\pi$-cloud interactions, and the other methane molecule is off the ring interacting primarily with the first methane, contributing little to the cluster spectral shift.

The overall behavior of this cluster system with regard to geometry, binding energy, and cluster population in the beam is very similar to that found for benzene, toluene and pyrazine methane species.[1-7]

B. Pyrimidine - Ethane.

The pyrimidine $(C_2H_6)_1$ cluster is similar to the pyrazine $(C_2H_6)_1$ cluster:[7] both clusters have three geometrical configurations and each configuration of the two clusters has a similar binding energy. These configurations are also similar to those of the benzene $(C_2H_6)_1$ cluster with the exception that, in the N-heterocyclic systems, two parallel orientations of the $C_2H_6$ long axis with respect to the ring plane are now possible.

The identification of calculated geometries with the three distinct spectroscopic features is of course tentative but can be pursued in the spirit of the arguments and correlations employed with the benzene and pyrazine systems.[1-7] Referring to figures 3 and 4, the feature at -71.4 $cm^{-1}$ can be associated with configuration I, the intense feature at -60.7 $cm^{-1}$ can be associated with configuration II, and the -52.7 $cm^{-1}$ feature is associated with configuration III. The lack of vdW vibronic structure for these transitions must be due to the similarity between the ground and excited state potentials for the clusters.

    C.  Pyrimidine - Ammonia.

    The pyrimidine $(NH_3)_1$ clusters have a unique spectrum which can only be interpreted as due to three distinct configurations with no vdW mode progression intensity following the well defined origins. Calculations, as pointed out previously, give exactly these conclusions and identification of origins in the spectrum with configurations seems straightforward. Configurations I and II of figure 6 are associated with the features at 366 and 368 $cm^{-1}$ in figure 5. These two configurations are quite similar and have less hydrogen bonding interaction than the more blue shifted single feature at 496 $cm^{-1}$. The large spectral blue shifts of ~365 and ~500 $cm^{-1}$ must arise from the strong hydrogen bonding interactions. While none of these observations seem particularly striking in and of itself, in comparison with the pyrazine $(NH_3)_1$ and benzene $(NH_3)_1$ results, they are surprising; these will be discussed below.

    D.  Pyrazine - Ammonia.

    The pyrazine $(NH_3)_1$ cluster spectrum is completely different from that of pyrimidine $(NH_3)_1$. The cluster $0^0_0$ is shifted +117 $cm^{-1}$ from the pyrazine $0^0_0$, only one cluster geometry is present, and a rather extensive vdW vibronic structure is built upon the origin. The $6a^1_0$ spectrum is quite similar. Two intense vdW vibronic transitions are associated with

14

these cluster transitions. The $10a_o^1$ vibration region of the pyrazine $(NH_3)_1$ cluster, on the other hand, looks quite different from these other features and vibronic interactions between the out of plane $10a^1$ carbon-carbon mode and the vdW modes are quite evident in the overall vibronic intensity pattern in the $10a_o^1$ region.

Calculations predict only one configuration for this cluster system. The fact that the potential energy calculations can accurately parallel the spectral data for pyrimidine and pyrazine ammonia clusters which are clearly so different, gives us a high degree of confidence in the calculational process, the binding energies, and the potential form accuracy.

E. Benzene - Ammonia.

Assignment of the benzene $(NH_3)_1$ spectra has not been attempted as yet because the spectra are too complicated. We present them only as part of the general picture indicating what spectra of relatively simple clusters of such systems can be like. The benzene $(NH_3)_1$ clusters yield much more complicated spectra than either pyrazine or pyrimidine $(NH_3)_1$ clusters do. In the benzene $(NH_3)_1$ cluster, strong vdW vibronic interactions must be important for the cluster transition intensity.

Both calculated configurations (figure 10) contribute to the $6_o^1$ transition but only configuration II generates the $0_o^o$ spectrum. Note too, that both configurations most likely generate a red shift.

F. Benzene - Water.

Any $C_6H_6(H_2O)_1$ cluster will in principle generate a $0_o^o$ transition. The $0_o^o$ spectrum of $C_6H_6(H_2O)_1$ (figure 11) thus strongly suggests that only one cluster geometry is realized for this system. The $C_6H_6(H_2O)_1$ $0_o^o$ transition is much like the pyrazine $(NH_3)_1$ spectrum. Well developed vdW vibronic features are observed. The $6_o^1$ spectrum implies strong vibronic mixing between the in plane carbon-carbon deformation $6^1$ and

the vdW bends and torsions:  the cluster shift is different for $6_0^1$, as is

the intensity pattern.  The cluster shift at the $0_0^0$ transition is $+85$ cm$^{-1}$

which indicates that the cluster excited state is destablized with respect to

the ground state.  The blue shift may be related to the unique hydrogen

bonding capabilities of the $H_2O$ molecule with the $\pi$-system of benzene.  The

calculated binding energy is probably ~50 cm$^{-1}$ low for this cluster because

the $6_0^1$ transition at $0_0^0$ plus 520 cm$^{-1}$ is observed.  We have previously

noted that the LJ potential binding energy is roughly 50 cm$^{-1}$ low compared

to exp-6 and experimental values.[7]

An infrared study of the 1:1 benzene-water complex in an argon matrix has

been reported.[23]  The work suggests that the water molecule hydrogen bonds

to the benzene $\pi$-system in a manner nearly identical to that found in the

calculations presented in figure 12.

V.  Conclusions.

The clusters studied in this work fall into two broad categories:  a

conventional set containing pyrimidine hydrocarbon clusters, the spectra of

which are quite similar to those of other aromatic and pyrazine hydrocarbon

systems, and benzene, pyrimidine, and pyrazine ammonia and benzene water

clusters, the spectra of which are all unique and surprisingly erratic.  In

the latter grouping, spectral cluster shifts range from -100 to +500 cm$^{-1}$,

vdW vibronic spectra range from nonexistent to intense, vdW modes can be highly

perturbing to the solute vibronic structure and energy, and the number of

cluster configurations varies from one to three in an apparently arbitrary

fashion.  These differences notwithstanding, the Lennard-Jones (6-12-1) poten-

tial, augmented appropriately with hydrogen bonding interactions (10-12) as

required, always gives geometry and binding energy results that are in complete

agreement with the spectra as far as the comparison can be made (i.e., symmetry,

numbers of configurations, red and blue shifts with regard to hydrogen bonding,

etc). The atom-atom LJ potential form has been chosen for these calculations because a large number of parameters for different types of atoms are available in the literature.

The benzene $(NH_3)_1$ and $(H_2O)_1$ spectra are quite different from one another. The shifts for these two clusters and their geometries seem to emphasize the importance of hydrogen bonding in the benzene $(H_2O)_1$ cluster.

Pyrazine and pyrimidine water clusters are not found in these studies although they have been extensively investigated. These clusters are not observed perhaps because their excited states are dissociative, but more likely because of rapid excited state intersystem crossing and/or internal conversion.

REFERENCES

1. M. Schauer and E.R. Bernstein, J. Chem. Phys. $\underline{82}$, 726 (1985).

2. M. Schauer, K.S. Law and E.R. Bernstein, J. Chem. Phys. $\underline{82}$, 736 (1985).

3. K.S. Law and E.R. Bernstein, J. Chem. Phys. $\underline{82}$, 2856 (1985).

4. K.S. Law, M. Schauer, and E.R. Bernstein, J. Chem. Phys. $\underline{81}$, 4871 (1984).

5. E.R. Bernstein, K. Law, and M. Schauer, J. Chem. Phys. $\underline{80}$, 207 (1984).

6. M. Schauer, K. Law, and E.R. Bernstein, J. Chem. Phys. $\underline{81}$, 49 (1984).

7. J. Wanna and E.R. Bernstein, J. Chem. Phys. $\underline{84}$, 927 (1986).

8. M.M. Carrabba, J.E. Kenny, W.R. Moomaw, J. Cordes, and M. Denton, J. Phys. Chem. $\underline{89}$, 674 (1985).

9. a. H. Abe, N. Mikami, and M. Ito, J. Phys. Chem. $\underline{86}$, 1768 (1982);

   b. H. Abe, N. Mikami, M. Ito, and Y. Udagawa, J. Phys. Chem. $\underline{86}$, 2567 (1982);

   c. K. Fuke, H. Yoshiuchi, K. Kaya, Y. Achiba, K. Sato, and K. Kimura, Chem. Phys. Lett. $\underline{108}$, 179 (1984);

   d. N. Gonohe, H. Abe, N. Mikami, and M. Ito, J. Phys. Chem. $\underline{89}$, 3642 (1985).

10. a. J. Hager and S.C. Wallace, J. Phys. Chem. $\underline{88}$, 5513 (1984);

    b. J. Hager and S.C. Wallace, J. Phys. Chem. $\underline{89}$, 3833 (1985).

11. D.E. Poeltl and J.K. McVey, J. Chem. Phys. $\underline{78}$, 4349 (1983).

12. a. C.A. Haynam, D.V. Brumbaugh, and D.H. Levy, J. Chem. Phys. $\underline{79}$, 1581 (1983);

    b. L. Young, C.A. Haynam, and D.H. Levy, J. Chem. Phys. $\underline{79}$, 1592 (1983).

13. G. Smulevich, A. Amirav, V. Even, and J. Jortner, Chem. Phys. $\underline{73}$, 1 (1982).

14. a. P.M. Felker, W.R. Lambert, and A.H. Zewail, J. Chem. Phys. $\underline{77}$, 1603(1982);

    b. L.A. Heimbrook, J.E. Kenny, B.E. Kohler, and G.W. Scott, J. Phys. Chem. $\underline{87}$, 280 (1983).

15. M. Kasha, Discuss. Faraday Soc. $\underline{9}$, 14 (1950).

16. a. F.A. Momany, L.M. Carruthers, R.F. McGuire, and H.A. Scheraga, J. Phys. Chem. $\underline{78}$, 1595 (1974);

    b. G. Nemethy, M.S. Pottle, and H.A. Scheraga, J. Phys. Chem. $\underline{87}$, 1883 (1983).

17.  a.  C.A. Haynam, D.V. Brumbaugh, and D.H. Levy, J. Chem. Phys. 80, 2256 (1984);

     b.  D.V. Brumbaugh, J.E. Kenny, and D.H. Levy, J. Chem. Phys. 78, 3415 (1983);

     c.  K.E. Johnson, W. Sharfih, and D.H. Levy, J. Chem. Phys. 74, 163 (1981);

     d.  K.E. Johnson, L. Wharton, and D.H. Levy, J. Chem. Phys. 69, 2719 (1978).

18.  K. Yamanouchi, H. Watanabe, S. Koda, S. Tsuchiya, and K. Kuchitsu, Chem. Phys. Lett. 107, 290 (1984).

19.  a.  P.J. Wheatley, Acta Cryst. 10, 182 (1957);

     b.  P.J. Wheatley, Acta Cryst. 13, 80 (1960).

20.  J.A. Menapace and E.R. Bernstein, J. Chem. Phys. to be published.

21.  a.  A.E.W. Knight, C.M. Lawburgh, and C.S. Parmenter, J. Chem. Phys. 63, 4336 (1975);

     b.  I. Knoth, H.J. Neusser and E.W. Schlag, J. Phys. Chem. 86, 891 (1982);

     c.  A.K. Jameson, H. Saigusa and E.C. Lim, J. Phys. Chem. 87, 3007 (1983);

     d.  H. Abe, Y. Ohyanagi, M. Ichijo, N. Mikami and M. Ito, J. Phys. Chem. 89, 3512 (1985).

22.  M.L. Sage and J. Jortner, J. Chem. Phys. 82, 5437 (1985).

23.  A. Engdahl and B. Nelander, J. Phys. Chem. 89, 2860 (1985).

Table I

Parameters for the energy expression in the computer modeling.

$$E_{ij} = 1.16 \times 10^5 \; q_i q_j / 2r_{ij} \; + \; A_{ij}/r_{ij}^{12} \; - \; C_{ij}/r_{ij}^6 \qquad (LJ)$$

$$A \left( \frac{cm^{-1} \; \overset{o}{A}^{12}}{mole} \right) \quad C \left( \frac{cm^{-1} \; \overset{o}{A}^{6}}{mole} \right)$$

Amine-Aromatic

| | | |
|---|---|---|
| N–N | $1.312 \times 10^8$ | $1.403 \times 10^5$ |
| N–C | $1.728 \times 10^8$ | $1.575 \times 10^5$ |
| N–H | $2.523 \times 10^7$ | $4.527 \times 10^4$ |
| H–C | $2.749 \times 10^7$ | $5.217 \times 10^4$ |
| H–H | $3.872 \times 10^6$ | $1.590 \times 10^4$ |
| H–N | $1.990 \times 10^7$ | $4.527 \times 10^4$ |

Water-Aromatic

| | | |
|---|---|---|
| O–N | $7.548 \times 10^7$ | $1.021 \times 10^5$ |
| O–C | $9.868 \times 10^7$ | $1.130 \times 10^5$ |
| O–H | $1.363 \times 10^7$ | $3.162 \times 10^4$ |
| H–C | $3.160 \times 10^7$ | $5.217 \times 10^4$ |
| H–H | $4.537 \times 10^6$ | $1.590 \times 10^4$ |
| H–N | $2.297 \times 10^7$ | $4.527 \times 10^4$ |

Table I (Cont)

$$E_{ij} = 1.16 \times 10^5 \; q_i q_j / 2r_{ij} \; + \; {A'}/r_{ij}^{12} \; - \; B/r_{ij}^{10} \quad \text{(HB)}$$

$$A' \left( \frac{cm^{-1} \; A^{o12}}{mole} \right) \qquad B \left( \frac{cm^{-1} \; A^{o10}}{mole} \right)$$

| | | | |
|---|---|---|---|
| H...N | | $1.150 \times 10^7$ | $2.882 \times 10^6$ |

| | | q |
|---|---|---|
| $NH_3$: | N | $-0.438$ |
| | H | $+0.146$ |
| $H_2O$: | O | $-0.34$ |
| | H | $+0.17$ |
| $C_4H_4N_4$: | N | $-0.182$ |
| | C | $+0.091$ |
| | H | $0$ |
| $C_6H_6$: | C | $-0.0074$ |
| | H | $+0.0074$ |

Table II

Observed peaks in the spectra of pyrimidine-methane clusters.

| Species | Energy (vac. cm$^{-1}$) | Energy Relative to Pyrimidine $0_0^0$ (cm$^{-1}$) | Energy Relative to Cluster $0_0^0$ (cm$^{-1}$) | Assignment[a] |
|---|---|---|---|---|
| $C_4H_4N_2(CH_4)_1$ | 31016.4 | -56.6 | 0 | $0_0^0$ |
| | 31020.9 | -52.1 | 4.5 | |
| $C_4H_4N_2(CH_4)_2$ | 30960.9 | -112.1 | 0 | iso $0_0^0$ |
| | 30966.0 | -107.0 | 5.1 | |
| | 31025.8 | -47.2 | 0 | aniso $0_0^0$ |

a) The -112.1 cm$^{-1}$ shift is associated with two methanes added symmetrically above and below the pyrimidine ring (isotropic), as shown in Figure 2. The -47.2 cm$^{-1}$ shift is associated with the anisotropic configuration, as shown in Figure 2.

Table III

Observed peaks in the spectra of pyrimidine-ethane clusters.

| Species | Energy | Energy Relative to Pyrimidine $0_0^0$ (cm$^{-1}$) | Energy Relative to Cluster $0_0^0$ (cm$^{-1}$) | Tentative Assignment |
|---|---|---|---|---|
| $C_4H_4N_2(C_2H_6)_1$ | 30919.5 | -153.5 | | |
| | 30973.7 | - 99.3 | | |
| | 30986.1 | - 86.9 | | |
| | 30997.6 | - 75.4 | | |
| | 31001.6 | - 71.4 | 0 | I $0_0^0$ |
| | 31012.3 | - 60.7 | 0 | II $0_0^0$ |
| | 31020.3 | - 52.7 | 0 | III $0_0^0$ |
| | 31033.9 | - 39.1 | 21.6 | II $16b_1^1$ |

Table IV

Pyrimidine $(NH_3)_1$

| Energy (vac. cm$^{-1}$) | Energy Relative to corresponding pyrimidine feature (cm$^{-1}$) | Energy Relative to corresponding pyrimidine-ammonia feature (cm$^{-1}$) | Assignment |
|---|---|---|---|
| 31378.2 | 305.2 | -60.9 | |
| 31439.1 | 366.1 | 0 | I $0_0^0$ |
| 31441.0 | 368.0 | 0 | II $0_0^0$ |
| 31485.7 | 412.7 | 46.6 | |
| 31520.0 | 447.0 | 80.9 | |
| 31535.2 | 462.2 | 96.1 | |
| 31561.3 | 488.3 | 122.2 | |
| 31568.9 | 495.9 | 0 | III $0_0^0$ |
| 31579.3 | 506.3 | 10.4 | |
| 31610.1 | 537.1 | 41.2 | |
| 31685.1 | 612.1 | 116.2 | |
| 32044.6 | 360.6 | 0 | I $6a_0^1$ |
| 32050.8 | 366.8 | 0 | II $6a_0^1$ |
| 32097.2 | 355.2 | 0 | I $6b_0^2$ |
| 32106.2 | | | |
| 32121.5 | 379.5 | 0 | II $6b_0^2$ |
| 32162.6 | | | |
| 32176.1 | 492.1 | 0 | III $6a_0^1$ |
| 32224.7 | 452.7 | 0 | III $6b_0^2$ |

## Table V

### Pyrazine $(NH_3)_1$

| Energy (vac. cm$^{-1}$) | Energy Relative to corresponding pyrazine feature (cm$^{-1}$) | Energy Relative to corresponding pyrazine-ammonia cluster (cm$^{-1}$) | Assignment |
|---|---|---|---|
| 30967.3 | 91.3 | -25.7 | |
| 30993.0 | 117.0 | 0 | $0_0^0$ |
| 31000.8 | 124.8 | 7.8 | |
| 31019.5 | 143.5 | 26.5 | |
| 31036.5 | 160.5 | 43.5 | |
| 31043.6 | 167.6 | 50.6 | |
| 31045.4 | 169.4 | 52.4 | |
| 31067.3 | 191.3 | 74.3 | |
| 31070.0 | 194.0 | 77.0 | |
| 31077.4 | 201.4 | 84.4 | |
| 31089.9 | 213.9 | 96.9 | |
| 31093.7 | 217.7 | 100.7 | |
| 31099.2 | 223.2 | 106.2 | |

## Table V

### Pyrazine $(NH_3)_1$ (continued)

| Energy (vac. $cm^{-1}$) | Energy Relative to corresponding pyrazine feature ($cm^{-1}$) | Energy Relative to corresponding pyrazine-ammonia feature ($cm^{-1}$) | Assignment |
|---|---|---|---|
| 31378.7 | 119.7 | 0 | $10a_0^1$ |
| 31384.9 | 125.9 | 6.2 | |
| 31400.5 | 141.5 | 21.8 | |
| 31403.7 | 144.7 | 25.0 | |
| 31424.3 | 165.3 | 45.6 | |
| 31441.8 | 182.8 | 63.1 | |
| 31461.3 | 202.3 | $(82.6)^a$ | |
| 31467.5 | 208.5 | (88.8) | |
| 31507.5 | 248.5 | 126.8 | |
| 31513.7 | 254.7 | 135.0 | |
| 31539.5 | 280.5 | 160.8 | |
| 31559.7 | 300.7 | 181.0 | |
| 31580.2 | 120.5 | 0 | $6a_0^1$ |
| 31590.8 | 131.1 | 10.6 | |
| 31624.8 | 165.1 | 44.6 | |

a  may be associated with other pyrazine features.

Table VI

Benzene $(H_2O)_1$

| Energy (vac. $cm^{-1}$) | Energy Relative to corresponding benzene feature ($cm^{-1}$) | Energy Relative to corresponding benzene-water feature ($cm^{-1}$) | Assignment |
|---|---|---|---|
| | | $0_0^0$ | |
| 38168.6 | 84.6 | 0 | |
| 38173.9 | 89.9 | 5.3 | |
| 38185.5 | 101.5 | 16.9 | |
| 38191.0 | 107.0 | 22.4 | |
| 38205.3 | 121.3 | 36.7 | |
| 38221.6 | 137.6 | 53.0 | |
| 38243.5 | 159.5 | 74.9 | |
| 38274.9 | 190.9 | 106.3 | |
| | | $6_0^1$ | |
| | | a | |
| 38655.4 | 48.4 | 0 | |
| 38656.8 | 49.8 | | |
| 38683.8 | 76.8 | 27.7 | |
| 38688.6 | 81.6 | 32.5 | |
| 38694.2 | 87.2 | 38.1 | |
| 38709.1 | 102.1 | 53.0 | |
| 38720.7 | 113.7 | 64.6 | |
| 38762.1 | 155.1 | 106.0 | |

a) shift taken with $6_0^1$ at 49.1

FIGURE CAPTIONS

Figure 1    Two-color time of flight mass spectra (2-color TOFMS) of
            pyrimidine $(CH_4)_1$ and pyrimidine $(CH_4)_2$ in the region
            of the pyrimidine origin (31073.0 $cm^{-1}$).

Figure 2    Minimum energy configurations and binding energies for
            pyrimidine $(CH_4)_1$ and pyrimidine $(CH_4)_2$ as obtained using
            the LJ potential calculation described in the text.

Figure 3    Two-color TOFMS of pyrimidine $(C_2H_6)_1$ in the region of the
            pyrimidine origin.

Figure 4    Minimum energy configurations and binding energies for
            pyrimidine $(C_2H_6)_1$ as obtained using a LJ potential
            calculation.

Figure 5    Two-color TOFMS of pyrimidine $(NH_3)_1$ in the region 300-500
            $cm^{-1}$ to the blue of the pyrimidine origin.  An insert is
            shown of the first two features with an expanded scale.

Figure 6    Minimum energy configurations and binding energies for
            pyrimidine $(NH_3)_1$ as obtained using a LJ plus HB potential
            calculation.

Figure 7    Two-color TOFMS of pyrazine $(NH_3)_1$ at the origin, $10a_0^1$ and
            $6a_0^1$ regions are shown.  The cluster origin (0 $cm^{-1}$) is
            +117 $cm^{-1}$ to the blue of the pyrazine origin.

PYRIMIDINE $(CH_4)_1$

PYRIMIDINE $(CH_4)_2$
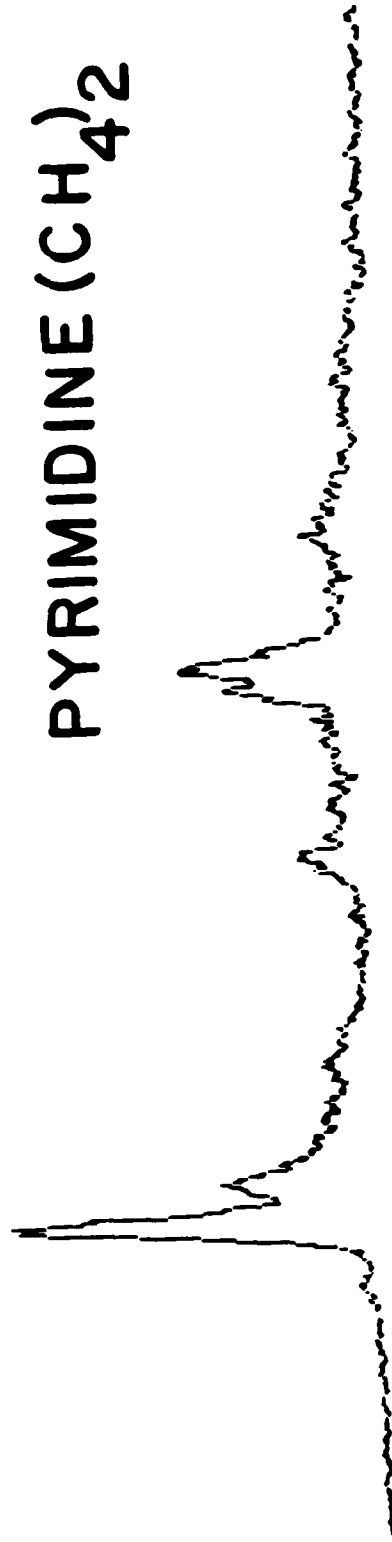
-100    -50    0
RELATIVE ENERGY ENERGY $(cm^{-1})$

PYRIMIDINE(CH₄)₂

PYRIMIDINE(CH₄)₁
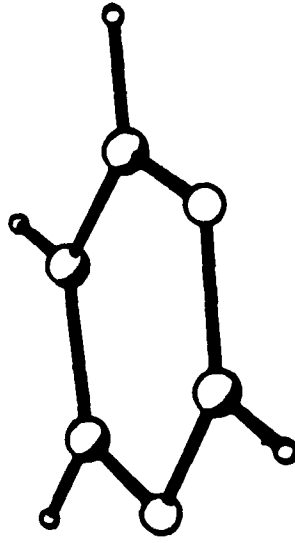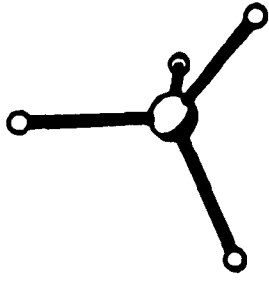
-879 cm⁻¹

-1029 cm⁻¹

-514 cm⁻¹
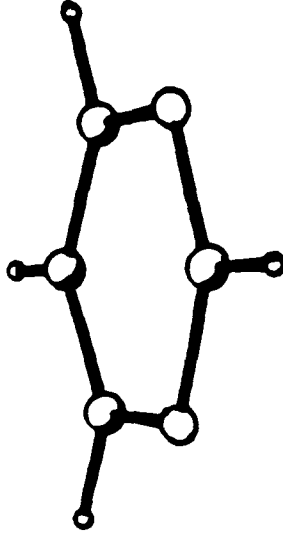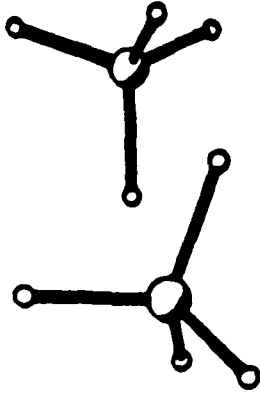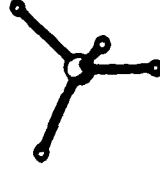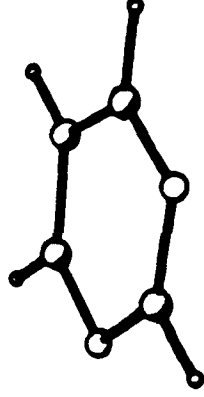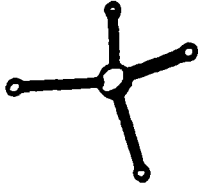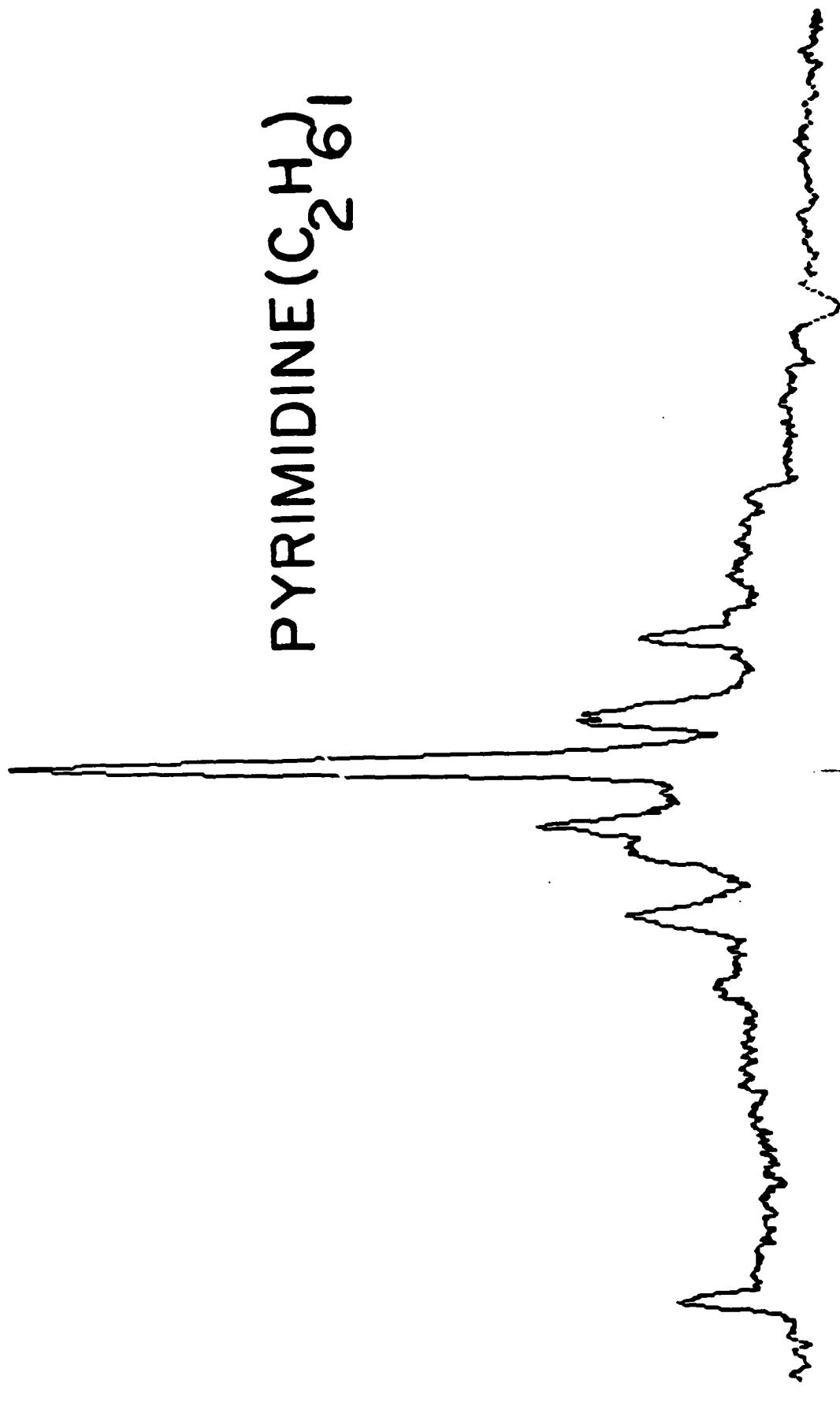
PYRIMIDINE $(C_2H_6)_1$

RELATIVE ENERGY $(cm^{-1})$

PYRIMIDINE $(C_2H_6)_1$
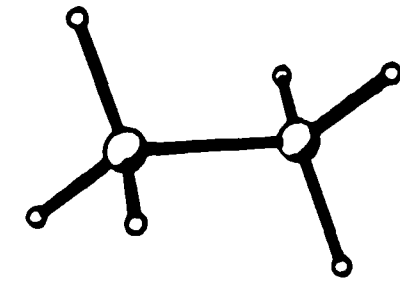
I  —566 cm$^{-1}$
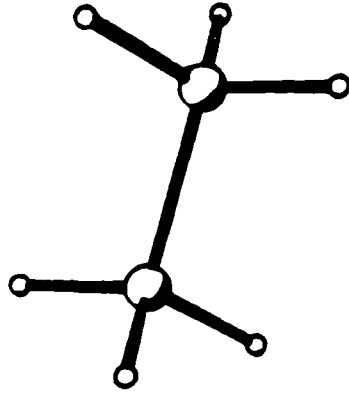
II  —669 cm$^{-1}$
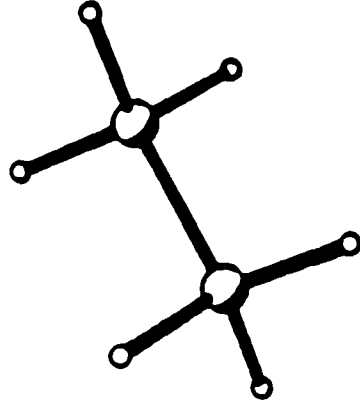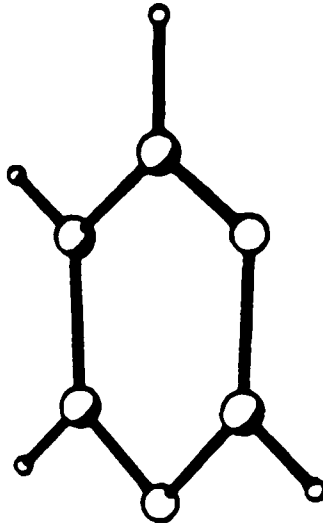
III  —676 cm$^{-1}$

PYRIMIDINE$(NH_3)_1$

I & II

III

RELATIVE ENERGY $(cm^{-1})$

+300    +350    +400    +450    +500
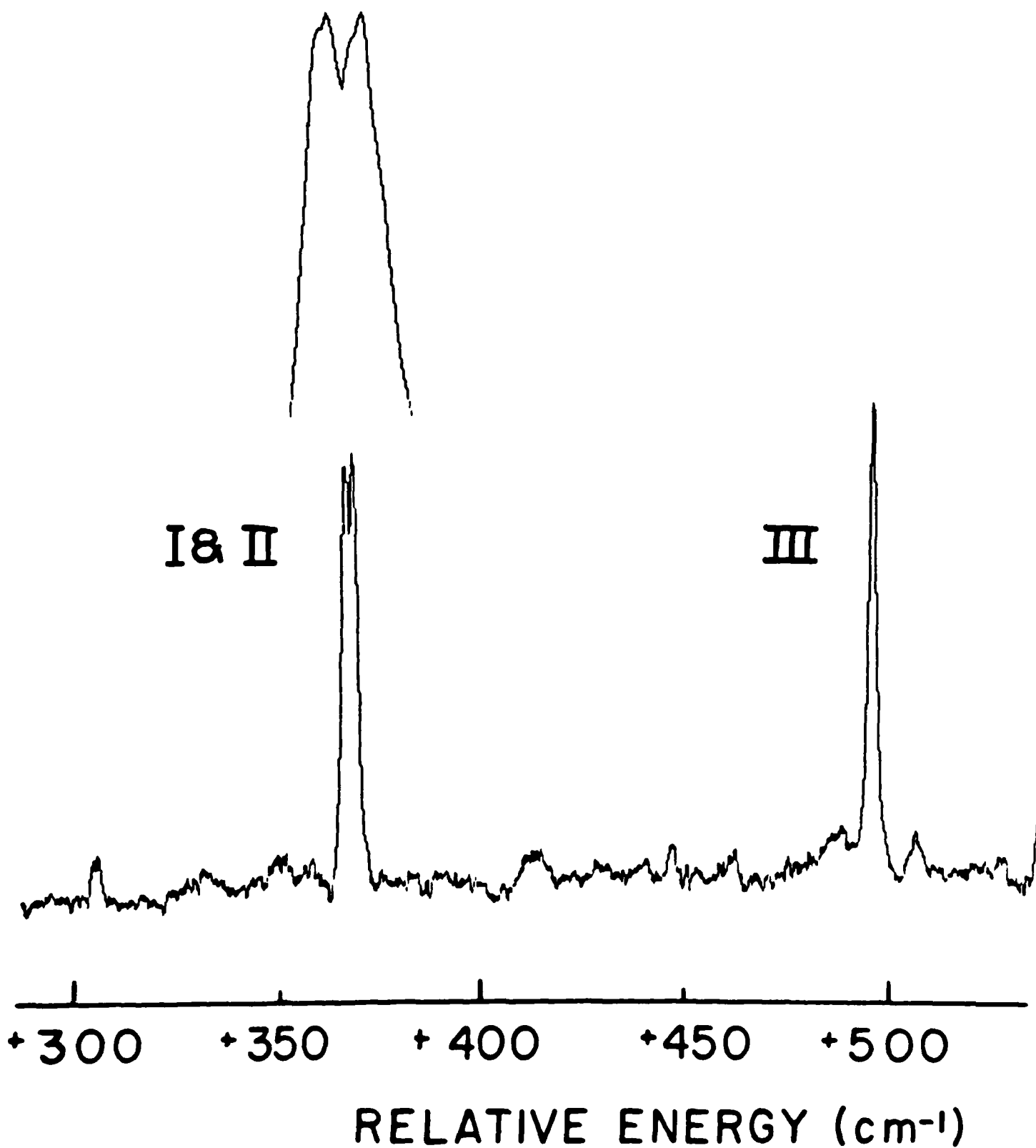
# PYRIMIDINE - AMMONIA
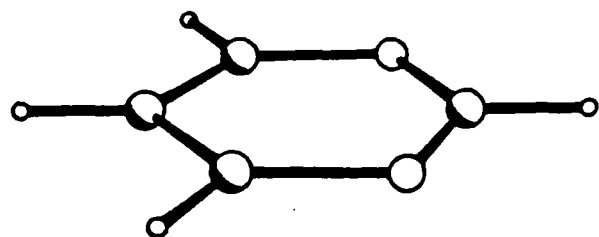


I    -689 cm⁻¹
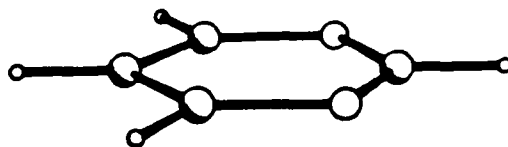
II   -667 cm⁻¹
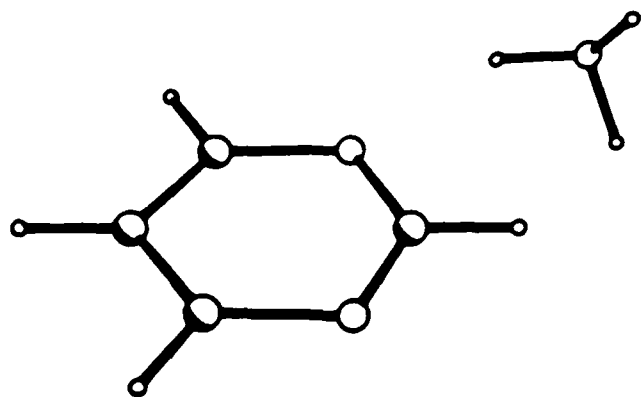
III  -537 cm⁻¹

PYRAZINE$(NH_3)_1$

$0^0_0$

$10a^1_0$

$6a^1_0$
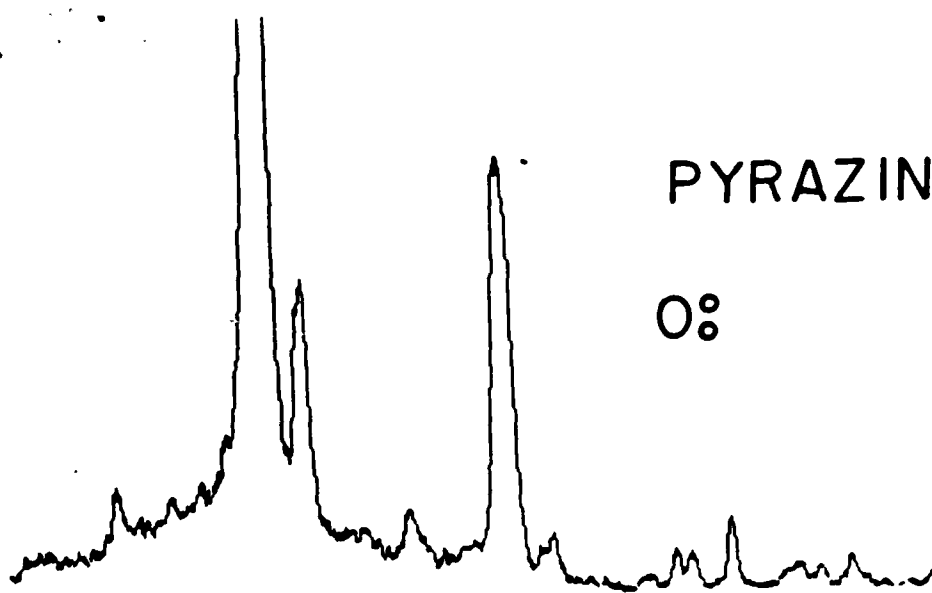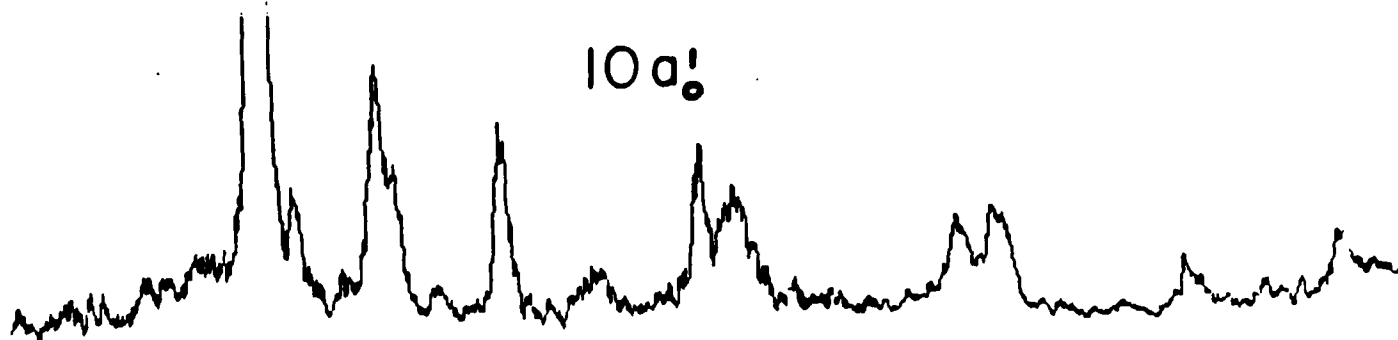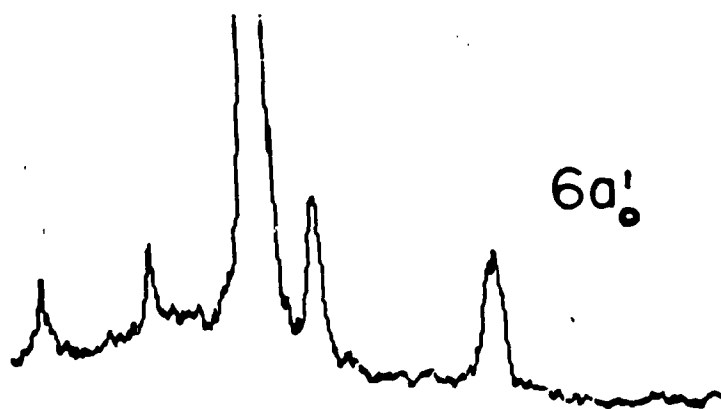
RELATIVE ENERGY $(cm^{-1})$

PYRAZINE - AMMONIA

−677 cm⁻¹

$C_6H_6(NH_3)_1$

$0_0^0$

$6_0^1$

II

18II
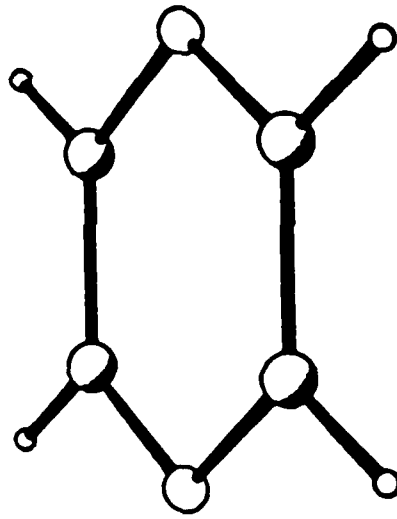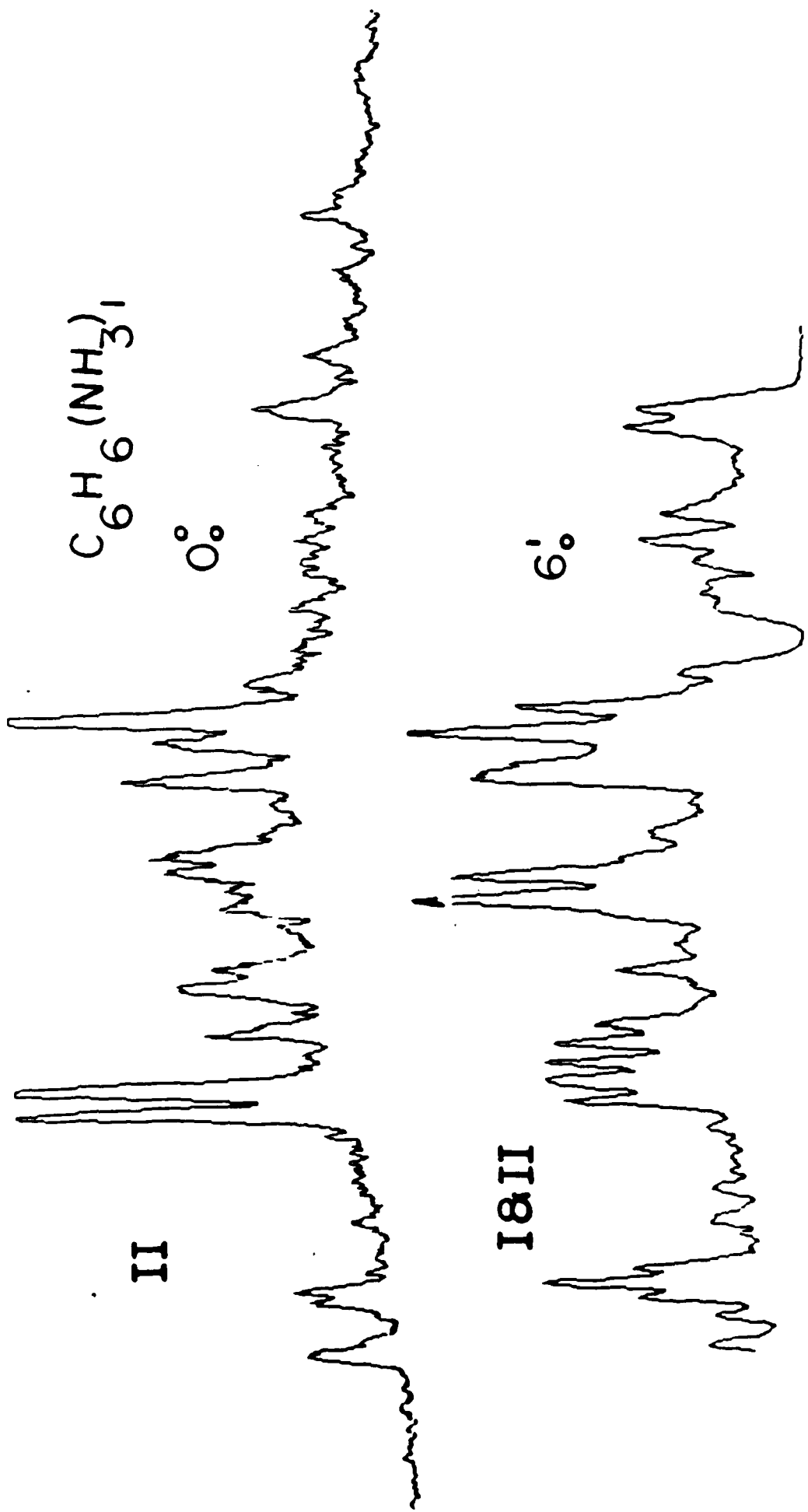
RELATIVE ENERGY (cm⁻¹)

BENZENE-AMMONIA

II  -608

I  -711

$C_6H_6(H_2O)_1$

$0^0_0$

$6^1_0$

RELATIVE ENERGY (cm$^{-1}$)

+50        +100        +150
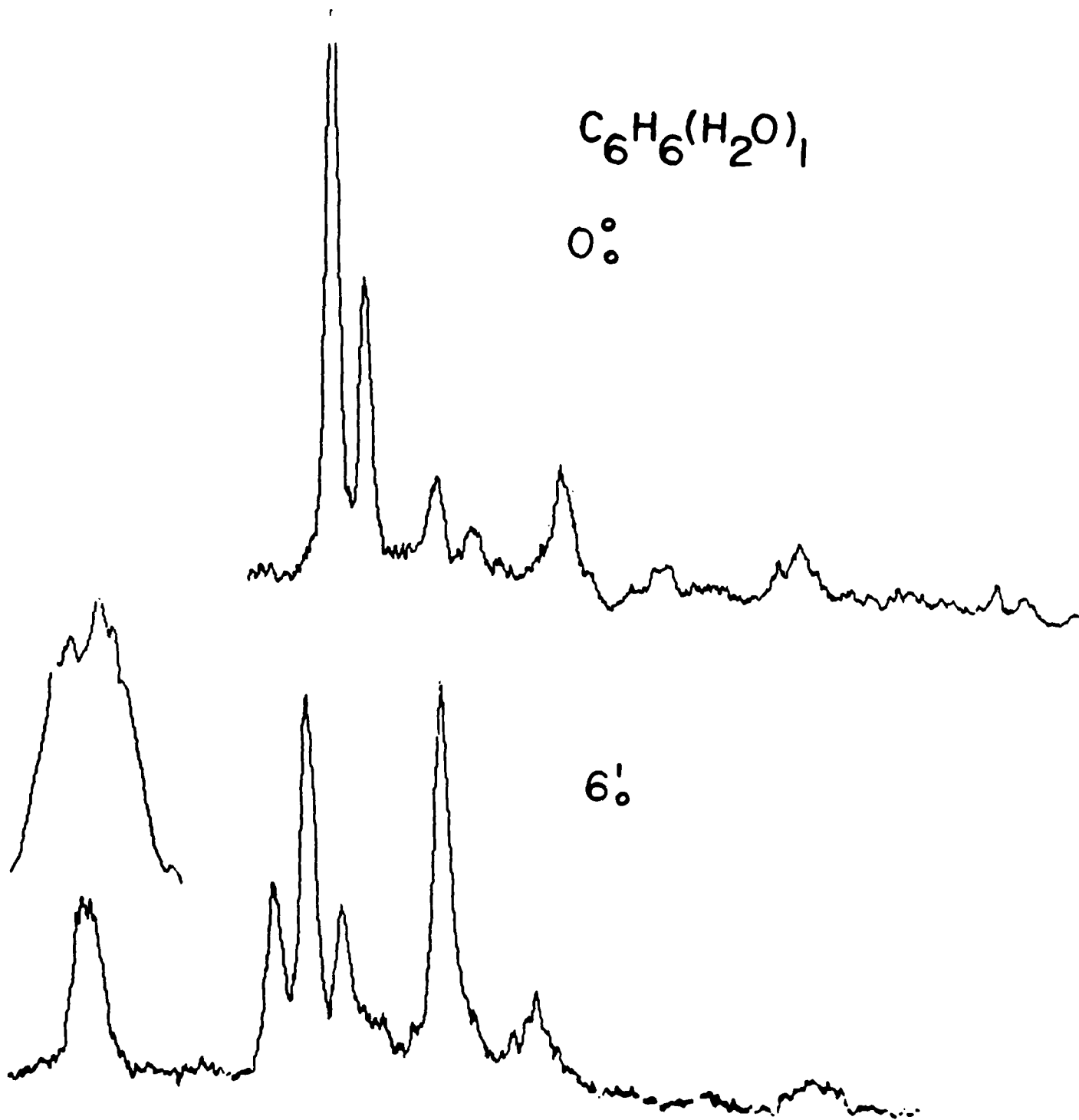
# BENZENE-WATER
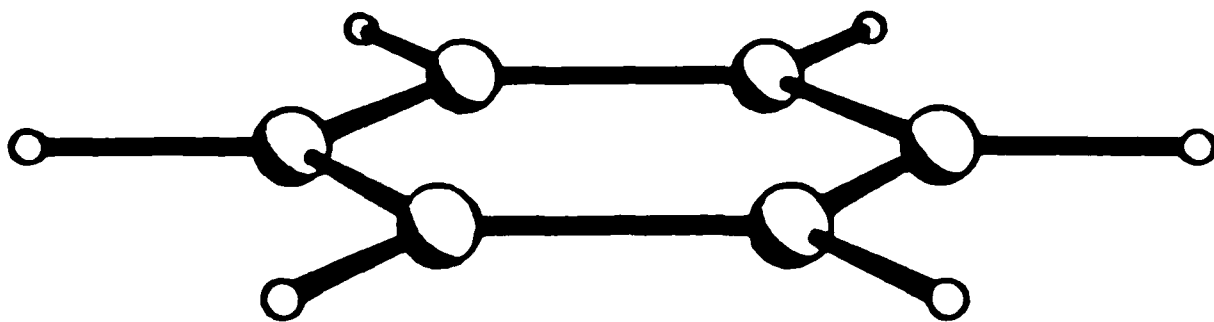


$-505$ cm$^{-1}$

TECHNICAL REPORT DISTRIBUTION LIST, GEN

|  | No. Copies |  | No. Copies |
|---|---|---|---|
| Office of Naval Research<br>Attn: Code 413<br>800 N. Quincy Street<br>Arlington, Virginia 22217 | 2 | Dr. David Young<br>Code 334<br>NORDA<br>NSTL, Mississippi 39529 | 1 |
| Dr. Bernard Douda<br>Naval Weapons Support Center<br>Code 5042<br>Crane, Indiana 47522 | 1 | Naval Weapons Center<br>Attn: Dr. A. B. Amster<br>Chemistry Division<br>China Lake, California 93555 | 1 |
| Commander, Naval Air Systems<br>Command<br>Attn: Code 310C (H. Rosenwasser)<br>Washington, D.C. 20360 | 1 | Scientific Advisor<br>Commandant of the Marine Corps<br>Code RD-1<br>Washington, D.C. 20380 | 1 |
| Naval Civil Engineering Laboratory<br>Attn: Dr. R. W. Drisko<br>Port Hueneme, California 93401 | 1 | U.S. Army Research Office<br>Attn: CRD-AA-IP<br>P.O. Box 12211<br>Research Triangle Park, NC 27709 | 1 |
| Defense Technical Information Center<br>Building 5, Cameron Station<br>Alexandria, Virginia 22314 | 12 | Mr. John Boyle<br>Materials Branch<br>Naval Ship Engineering Center<br>Philadelphia, Pennsylvania 19112 | 1 |
| DTNSRDC<br>Attn: Dr. G. Bosmajian<br>Applied Chemistry Division<br>Annapolis, Maryland 21401 | 1 | Naval Ocean Systems Center<br>Attn: Dr. S. Yamamoto<br>Marine Sciences Division<br>San Diego, California 91232 | 1 |
| Dr. William Tolles<br>Superintendent<br>Chemistry Division, Code 6100<br>Naval Research Laboratory<br>Washington, D.C. 20375 | 1 | | |

ABSTRACTS DISTRIBUTION LIST, 051A

Dr. M. A. El-Sayed
Department of Chemistry
University of California
Los Angeles, California 90024

Dr. E. R. Bernstein
Department of Chemistry
Colorado State University
Fort Collins, Colorado 80521

Dr. J. R. MacDonald
Chemistry Division
Naval Research Laboratory
Code 6110
Washington, D.C. 20375

Dr. G. B. Schuster
Chemistry Department
University of Illinois
Urbana, Illinois 61801

Dr. W. M. Jackson
Department of Chemistry
Howard University
Washington, D.C. 20059

Dr. M. S. Wrighton
Department of Chemistry
Massachusetts Institute of Technology
Cambridge, Massachusetts 02139

Dr. A. Paul Schaap
Department of Chemistry
Wayne State University
Detroit, Michigan 49207

Dr. Gary Bjorklund
IBM
5600 Cottle Road
San Jose, California 95143

Dr. G. A. Crosby
Chemistry Department
Washington State University
Pullman, Washington 99164

Dr. W. E. Moerner
I.B.M. Corporation
5600 Cottle Road
San Jose, California 95193

Dr. Theodore Pavlopoulos
NOSC
Code 5132
San Diego, California 91232

Dr. D. M. Burland
IBM
San Jose Research Center
5600 Cottle Road
San Jose, California 95143

Dr. John Cooper
Code 6170
Naval Research Laboratory
Washington, D.C. 20375

Dr. George E. Walrafen
Department of Chemistry
Howard University
Washington, D.C. 20059

Dr. Joe Brandelik
AFWAL/AADO-1
Wright Patterson AFB
Fairborn, Ohio 45433

Dr. Carmen Ortiz
Consejo Superior de
    Investigaciones Cientificas
Serrano 117
Madrid 6, SPAIN

Dr. John J. Wright
Physics Department
University of New Hampshire
Durham, New Hampshire 03824

Dr. Kent R. Wilson
Chemistry Department
University of California
La Jolla, California 92093

# END

10 — 86

DTC